

DOI: <https://doi.org/10.1016/j.biortech.2017.02.129>

© 2017. This manuscript version is made available under the CC-BY-NC-ND 4.0 license [https://creativecommons.org/licenses/by-nc-nd/4.0/\(opens in new tab/window\)](https://creativecommons.org/licenses/by-nc-nd/4.0/(opens in new tab/window))

1 **Title(s)**

2 Analysis of the effect of temperature and reaction time on yields, compositions and oil quality in
3 catalytic and non-catalytic lignin solvolysis with formic acid using experimental design.

4 **Abstract**

5 The catalytic solvolysis of Norway spruce lignin in a formic acid/water media using bifunctional
6 Ru/Al₂O₃, Rh/Al₂O₃, Pd/Al₂O₃ catalysts was explored in a batch set-up at different temperatures and
7 reaction times (283-397°C and 21 min-11 h 40 min, respectively). Blank experiments using only
8 gamma-alumina as catalysts and non-catalyzed experiments were also performed and compared
9 with the supported catalysts results. Surface response methodology (RSM) and principal component
10 analysis (PCA) were used to evaluate the influence of the reaction conditions and type of system on
11 the oil yield, solid residue yield, oil quality and composition. The optimum reaction conditions were
12 found to be around 340°C and 6 h using Ru/Al₂O₃ as a catalyst; where nearly complete conversion of
13 lignin into oil is achieved (83.8 %) while still having high H/C ratios (1.21) coupled with low O/C ratios
14 (0.19) and *M_w* values (500 Da). No correlations between the oil yield and the quality of the oil has
15 been found. The oil yield is strongly dependent on the presence of the catalyst, temperature and
16 reaction time; while the oil quality is mainly dependent on reaction conditions. The recycling of the
17 catalyst proves that the deactivation of the Ru/Al₂O₃ catalyst is negligible after two separate recycling
18 tests. The results show the potential for improving the yields of oil by the use of catalysts which are
19 easily recovered, and suggest a good potential for tuning the oil composition to specific composition
20 depending on the requirements for the product.

21 **Introduction**

22 Global warming, volatile oil prices and world political instability point toward the necessity of new
23 localized and environmentally friendly ways of producing fuels and oil derived products from non-
24 alimentary sources [1, 2]. The development of economically feasible biomass-based bio-refineries is
25 recognized as one of the best alternatives to meet all these ongoing challenges [3]. Among the
26 biomass sources, lignocellulosic biomass (wood, grasses and agricultural residues) has been identified
27 as a promising resource for this purpose [4], since unlike vegetable oil and sugar crops, the
28 lignocellulose feedstocks avoid the negative side effect of intense farming [5] and ethical concerns
29 about the use of food as fuel raw materials [6].

30 Extensive work has been done on the chemical and enzymatic fractionation of lignocellulose, and the
31 subsequent conversion of the cellulose and hemicellulose fractions into bioethanol [6-10]. However,
32 the third component, lignin, comprising between 10-30 % of the feedstock, is mostly considered to
33 be a waste [11]. Several thermochemical processes have been explored as suitable for the conversion

34 of lignin-rich residual materials into fuels or phenols [4, 12-14]. A promising and relatively new lignin
35 conversion approach, known as lignin-to liquids (Ltl), involves the use of formic acid (FA) together
36 with a solvent. The solvent can be either ethanol or water, though the latter is preferred due to its
37 lower cost and more green nature. High oil yields, with high H/C and low O/C ratios are obtained, still
38 retaining the phenol-type structure of the bio- oil components. Therefore this versatile process can
39 be used for the production of both a bio-oil that can be blended with conventional fuels and to
40 produce aromatic compounds such as phenol, catechol and guaiacol [15, 16].

41 One of the major research challenges of the Ltl method is to obtain high oil yields and good quality
42 while decreasing the temperature and the reaction time of the process. Good oil quality can be
43 defined as a high energy content, stable, non-acidic and low viscous oils [17], with high H/C and low
44 O/C ratios and low average molecular weight distribution (M_w). One alternative to address this
45 challenge is the use of a catalyst in order to increase the lignin conversion rate[18]. Previously in our
46 group, Ru/Al₂O₃ (Ru), Rh/Al₂O₃ (Rh) and Pd/Al₂O₃ (Pd) have been shown to be an active catalyst
47 toward the conversion of lignin with formic acid in an aqueous media [19]. Among other aspects the
48 activity of the alumina support and the influence of the type of noble metal in the oil quality and
49 yield were discussed. However, the results found are not conclusive since those effects were mainly
50 studied only at a specific reaction condition, i.e. 340°C during 6 h.

51 A more systematic approach based on experimental design can be used, not only to confirm the
52 effect of the alumina support and type of noble metal in the oil yield and quality in a wider
53 experimental space, but also to address other aspects that could be interesting from an industrial
54 perspective: (i) the optimal reaction conditions, (ii) possible correlations between the oil yield and
55 the oil quality, (iii) the influence of reaction temperature and time in the composition of the oil, (iv)
56 activity of the catalysts upon recycling.

57 Here, a step-wise approach based on experimental design will be presented. Initially the effect of the
58 temperature (300-380°C) and reaction time (2-10 h) for three different catalytic systems (Ru, Rh, Pd)
59 will be evaluated using a full factorial design. Response surface methodology (RSM) and principal
60 component analysis (PCA) [17, 20] will be used to evaluate the influence of the reaction conditions
61 and type of catalyst on the oil yield, solid residue yield, oil quality and composition. An additional aim
62 of this screening study is to assess the similarities and differences within the catalytic systems.

63 In a second step, the influence of temperature (283-397°C) and reaction time (21 min-11h and 40
64 min) on three different reaction systems (non-catalyzed (NC), γ -Al₂O₃ (Al) and Ru catalyzed systems)
65 will be studied based on a central composite design [21]. Again RSM and PCA will be used to evaluate
66 the influence of the reaction conditions and type of system on the oil yield, solid residue yield, oil

67 quality and composition. In addition, the role of the noble metal and the γ -alumina support in the
68 lignin de-polymerization and hydrodeoxygenation will be evaluated.

69 In a third step, the activity of one of the catalysts will be evaluated upon two recycling cycles in terms
70 of oil yield and quality.

71

72 **2. Materials and Methods**

73 **2.1 Chemicals**

74 Formic acid (>98%), tetrahydrofuran (>99.9%) and ethyl acetate (99.8%) were purchased from Sigma
75 Aldrich and used as supplied. Lignin from Norway spruce (*Picea abies L.*) from strong acid
76 carbohydrate dissolution pre-treatment was received from Technical College of Bergen. The lignin
77 was ground, sieved (<500 μ m) and dried at 80°C for 24 h prior to use.

78 **2.2 Catalysts**

79 Ruthenium on alumina (5 wt%), Rhodium on alumina (5wt%), and Palladium on alumina (10 wt%),
80 were obtained from Sigma Aldrich, and gamma-alumina (97 wt%) was obtained from Strem
81 Chemicals Inc. These were dried at 80°C for 24 h prior to use.

82 **2.3 Catalyst characterization**

83 The type of acidity (Lewis or Brønsted), the total acidity, the acidity retention and the active acidity of
84 the Ru/Al₂O₃, Rh/Al₂O₃, Pd/Al₂O₃ and γ -alumina catalysts were analysed by NH₃-TPD and DRIFT of
85 absorbed pyridine. The active acidity is defined as the fraction of total acidity that actually plays a
86 significant role in the reaction (active acidity (T) = acidity retention (T) x total acidity).

87 Temperature-programmed desorption of ammonia, NH₃-TPD, was performed to determine the total
88 acidity of the samples. The measurements were carried out in a chemisorption analyzer AutoChem II
89 equipped with a thermal conductivity detector (Micromeritics, USA). A detailed description of the
90 analysis procedure is given elsewhere by Oregui Bengoechea *et al.* [19].

91 Diffuse reflectance infrared Fourier transform, DRIFT, was used to distinguish Lewis and Brønsted
92 acid sites of noble-metal containing catalysts and γ -Al₂O₃. The analyses were done using a VERTEX 70
93 spectrometer coupled with an external sample chamber that enables measurements under vacuum
94 (Bruker, Germany). A detailed description on the analysis procedure is given elsewhere by Oregui
95 Bengoechea *et al.* [19].

96 **2.4 Experimental conditions**

97 **2.4.1 Experimental set-up**

98 A detailed description is given elsewhere by Oregui Bengoechea *et al.* [19]. Briefly summarised, lignin
99 (2g), formic acid (3.075g), water (5g) and the catalyst (0.2g) were added to a stainless steel reactor
100 (Parr 4742 non-stirred reactor, 25 ml volume). The amounts of reactants are based on previous
101 experiments for maximising oil yields. The reactor was closed and heated in a Carbolite LHT oven up
102 to the desired conditions (283-397°C) for a given reaction time (21 min-11 h 40 min).

103 **2.4.2 Sample work-up**

104 A detailed description is given elsewhere by Oregui Bengoechea *et al.* [19]. Briefly summarized, after
105 the reactor was cooled down to the ambient temperature the produced gas was vented and the gas
106 quantity was determined. The reactor was opened and the liquid reaction mixture was extracted
107 with a solution of ethyl acetate: tetrahydrofuran (90:10). The solid phase (unreacted lignin, reaction
108 products and catalyst) was filtered and dried at ambient conditions for 2 days before weighing. Two
109 well-separated liquid phases were obtained (organic top phase and aqueous bottom phase). The
110 phases were separated by decantation and the organic phase was dried over Na₂SO₄ and
111 concentrated at reduced pressure (ca. 250 mmbar) at 40°C. The final oil and solid yield was
112 determined by weight (amount of oil/char (g.)/amount of introduced lignin (g.)). The solid yield for
113 the catalyzed systems is calculated after subtracting the amount of catalyst introduced. Therefore
114 the solid yield refers to the organic solids (char) and the inorganic lignin ashes.

115 **2.4.3 Recycling of the catalyst**

116 **2.4.3.1 Ash content of lignin**

117 Three crucibles were calcined at 575°C and weighted to the nearest 0.1 mg until constant weight
118 (less than ±0,3 mg after one 1 h of heating at 575°C). Once the weight of each crucible is recorded,
119 between 0.5 and 2.0 g. of lignin was weighed into each tared crucible. The lignin was calcined using
120 the following temperature programme: hold the temperature at 105°C for 12 min, increase the
121 temperature until 250°C at 10°C/min, hold the temperature at 250°C for 30 min, increase the
122 temperature until 575°C at 20°C/min, and hold it at that temperature for 180 min. After cooling, the
123 samples were weighed to the nearest of 0.1 mg weighted until constant weight. The final ash content
124 is calculated as the mean of the three crucibles.

125 **2.4.3.2 Recycling procedure**

126 The residual solids recovered after the work-up described in Section 2.4.2, were subjected to a
127 thermal treatment at 360°C for two hours with a heating ramp of 2°C/min to eliminate the organic
128 (char) residues. After the thermal treatment the resulting solids, catalyst and ashes, were re-used at
129 340°C and 6 h following the experimental set-up described in Section 2.4.1. The oil and solid yields
130 were calculated by weight and the oil was analysed. This procedure was repeated again to evaluate
131 the activity of the catalyst upon two recycling-cycles.

132

133 2.5 Characterization of the oils

134 2.5.1 GC-FID analysis

135 A detailed description is given elsewhere by Oregui Bengoechea *et al.* [19]. Briefly, the samples were
136 first silylated with BSTFA prior to the GC-FID analysis. The samples were analysed on a Thermo
137 Finnigan TRACE GC Ultra with a FID-detector equipped with a chromatographic HP-ULTRA2 column
138 from Agilent Technologies. The following heating programme was applied: 30°C for one minute, and
139 then heating at 10°C/min up to 25°C. The injector temperature was 250°C, and the detector
140 temperature was 320°C. Identification of the peaks was made by comparison with retention times of
141 authentic commercially available reference compounds that were also silylated prior to the analysis.
142 The quantitative data was obtained using hexadecane as internal standard. Calibration curves were
143 prepared for the following compounds: phenol (Ph), cresol (Cr), guaiacol (Gu), methyl-guaiacol (M-
144 Gu), catechol (Ca) and syringol (Sy), and their concentrations were calculated as % weight in the oil.

145 2.5.2 Elemental analysis

146 All samples were analysed for their elemental composition in the CHNS mode with a Vario EL III
147 instrument using helium as carrier gas. The amount of oxygen was calculated by difference.

148 2.5.3 GPC-SEC

149 The sample (1 mg) was dissolved in 1 mL of THF. The solution (20 µL) was injected into a GPC-SEC
150 system equipped with a PLgel 3µm Mini MIX-E column, and analysed at a flow rate of 0.5 mL/min of
151 THF at 21.1°C, and the detection was performed with UV at 254 and 280 nm, as well as with RI. The
152 set of columns was calibrated with a series of polystyrene standards covering a molecular-mass
153 range of 162–2360 Da.

154 2.6 Data analysis

155 2.6.1 Screening Experiments

156 A two-level full-factorial design with three center points was used to evaluate the influence of the
157 temperature (x_1) and reaction time (x_2) in each of the three different catalytic systems. The
158 experimental design was done separately for each catalytic system and different responses were
159 examined: oil and solid yield, H/C and O/C ratio, average molecular weight distribution (M_w) and oil
160 composition (see Section 2.6.1). The selected control variables (temperature and reaction time) and
161 their levels for each system are described in Table 1. The relation between the coded and the actual
162 values is the following:

$$163 \quad x_i = \frac{X_i - X_0}{\Delta X}$$

164 Where X_i is the actual value of the variable, X_0 is the actual value of X_i at the center point, and ΔX is
 165 the step change of the variable.

166 Table 1: experimental design for catalyst screening

Experiment	X_1		X_2	
	Temperature (°C)	Reaction time (h)	Actual	Coded
X^a-1	300	-1	10	+1
X^a-2	380	+1	10	+1
X^a-3	300	-1	2	-1
X^a-4	380	+1	2	-1
X^a-5	340	0	6	0
X^a-6	340	0	6	0
X^a-7	340	0	6	0

167 a) X : refers to either Ru (Ru/Al₂O₃ catalyst), Rh (Rh/Al₂O₃ catalyst) or Pd (Pd/Al₂O₃ catalyst)

168 2.6.1.1 Response surface methodology (RSM) for the oil and solid yield

169 Response Surface Methodology (RSM) is a set of mathematical and statistical techniques that can be
 170 used to define the relationships between the response and the independent variables, and the
 171 objective is to maximize this response [17, 22]. In the present study oil and solid yields were selected
 172 as response variables and fitted in a linear regression model with an interaction factor in the form of
 173 a polynomial equation:

$$174 Y = \beta_0 + \sum \beta_i x_i + \sum \sum \beta_{ij} x_i x_j \quad (1)$$

175 Where Y is the predicted response variable (oil or solid yield); β_0 , β_i , β_{ij} are constant regression
 176 coefficients of the model; and x_i , x_j ($ij= 1,2; i \neq j$) represent the coded values of independent variables
 177 that are used in statistical calculations. For each system separate oil and solid regression models
 178 were calculated and their response surface model built. After the regression model was obtained,
 179 the significance of the regression model was evaluated by the analysis of variance (ANOVA) [23-25].

180 2.6.1.2 Principal component analysis (PCA) to evaluate the quality of the oil

181 Principal component analysis (PCA) is a commonly used technique in statistics for simplifying the data
 182 by reducing multivariable to a 2-D plot in order to characterise the results. The use of principal
 183 component analysis allows identifying the factors which influence the data so that relationship can
 184 be established on a qualitative analysis. PCA uses complex matrix transformation which does not
 185 impose fixed vectors, and is completely dependent on the data set [26]. PCA has been used in the
 186 past to discriminate the effect of reaction conditions and reactant compositions in the quality of the
 187 LtL oils [5]. In the present study, the variables studied to evaluate the quality of the oils are: reaction
 188 temperature, reaction time, type of catalyst, oil and solid yield, H/C and O/C ratio of the oil and

189 average molecular weight distribution (M_w). The variable named catalyst is added to visualize the
 190 effect of the type of catalyst. This is a three level variable where Ru is represented by the coded level
 191 +1, Rh by 0, and Pd by -1. No cross-term is considered in this analysis to maximize the explained
 192 variance.

193 2.6.1.3 Principal component analysis (PCA) to evaluate the oil composition

194 Eight variables were submitted to PCA analysis. Three process variables, reaction temperature,
 195 reaction time and type of catalyst; and five response variables, named concentration of phenol (Ph),
 196 guaiacol (Gu), catechol (Ca), cresol (Cr) and methyl-guaiacol (M-Gu) in the oils. No cross-term is
 197 considered in the analysis to maximize the explained variance.

198 2.6.2 Optimization experiments

199 A central composite design (CCD) with axial ($\alpha=1,41$) and three centre points was used to evaluate
 200 the influence of the temperature (x_1) and reaction time (x_2) in three different reaction systems (NC:
 201 the non-catalysed system, Al: the γ -alumina system and the Ru system). The Ru system represents
 202 the best catalytic system in terms of oil yield. CCD allows determining both linear and quadratic
 203 models and is a good alternative of a three level full factorial design as it provides comparable results
 204 with smaller number of experiments [27]. The experimental design was carried out separately for
 205 each catalytic system and different responses were examined: oil and solid yield, H/C and O/C ratio,
 206 and M_w and oil composition (see Section 2.6.1). The selected control variables (temperature and
 207 reaction time) and their levels for each system are described in Table 2. The relation between the
 208 coded and the actual values is the following:

$$209 \quad x_i = \frac{X_i - X_0}{\Delta X}$$

210 Where X_i is the actual value of the variable, X_0 is the actual value of X_i at the centre point, and ΔX is
 211 the step change of the variable. For each system separate oil and solid regression models were
 212 calculated and their response surface model was built. After the regression model of experimental
 213 data was obtained, the significance of the regression model was evaluated by the analysis of variance
 214 (ANOVA) [23-25].

215 Table 2: experimental design for system optimization

Experiment	X_1		X_2	
	Temperature (°C)		Reaction time (h)	
	Actual	Coded	Actual	Coded
X-1	300	-1	10	+1
X-2	380	+1	10	+1
X-3	300	-1	2	-1

X-4	380	+1	2	-1
X-5	340	0	6	0
X-6	340	0	6	0
X-7	340	0	6	0
X-S1	397	+1.41	6	0
X-S2	283	-1.41	6	0
X-S3	340	0	21 min	-1.41
X-S4	340	0	11 h 40 min	+1.41

216 **X:** refers to either the Ru catalyzed system (Ru), γ -Al₂O₃ catalyzed system (Al) or the non-catalyzed
 217 system (NC) **S:** refers to the axial points were $\alpha=1,41$

218 2.6.2.1 Response surface methodology (RSM) for the oil and solid yield

219 In the present study oil and solid yields were selected as response variables and fitted to a second-
 220 order (quadratic) model in the form of quadratic polynomial equation:

$$221 Y = \beta_0 + \sum \beta_i x_i + \sum \beta_{ii} x_i^2 + \sum \sum \beta_{ij} x_i x_j \quad (2)$$

222 Where Y is the predicted response variable (either oil or solid yield); $\beta_0, \beta_i, \beta_{ii}, \beta_{ij}$ are constant
 223 regression coefficients of the model; and x_i, x_j ($ij= 1,2; i \neq j$) represent the coded values of
 224 independent variables that are used in statistical calculations. For each system separate oil and solid
 225 second order regression models were calculated and their response surface model was built. After
 226 the regression model of experimental data was obtained, the significance of the regression model by
 227 analysis of variance (ANOVA).

228 2.6.2.2 Principal component analysis (PCA) to evaluate the quality of the oil

229 The variables studied to evaluate the quality of the oils are: reaction temperature, reaction time,
 230 type of system, oil and char yield, H/C and O/C ratio of the oil and average molecular weight
 231 distribution (M_w). The variable named system is added to visualize the effect of the type of system.
 232 This is a three level variable where Ru is represented by the coded level +1, NC by 0, and Al by -1. No
 233 cross or quadratic term is considered in the analysis to maximize the explained variance.

234 2.6.2.3 Principal component analysis (PCA) to evaluate the oil composition

235 Initially eight variables were submitted to PCA analysis. Three process variables, reaction
 236 temperature, reaction time and type of system; and five response variables, named concentration of
 237 Ph, Gu, Ca, Cr and M-Gu in the oils (see Section 2.5.1). No cross or quadratic term is considered in
 238 either analysis to maximize the explained variance.

239

240 **3. Results and Discussion**

241 **3.1 Acidity Results of Ru/Al₂O₃, Rh/Al₂O₃, Pd/Al₂O₃ and γ -alumina**

242 Table 3 summarizes the results obtained for the DRIFT and NH₃-TPD analysis. IR bands assigned to
243 Brønsted acid sites (1545 and 1638 cm⁻¹) were not detected in any of the samples[28], suggesting
244 that only Lewis acidity (1448 cm⁻¹) is present (see *Figure S1, Supplementary Information*).

245 The highest total acidity measured by NH₃-TPD was obtained for the γ -Al₂O₃ (1.51 mmol NH₃/g
246 catalyst), with significantly lower acidities for the supported catalysts (Rh/Al₂O₃ > Ru/Al₂O₃ >
247 Pd/Al₂O₃). Based on the IR band at 1445 cm⁻¹, acidity retention was also calculated as [peak area (T) /
248 peak area (100°C)] x 100 (Table 3). Increasing the temperature did not influence the Lewis acid-
249 bound pyridine in Al₂O₃ and Pd/Al₂O₃, but caused pyridine desorption in the case of Rh/Al₂O₃ and
250 Ru/Al₂O₃. This suggests that the Lewis sites present in Rh/Al₂O₃ and Ru/Al₂O₃ samples are rather
251 weak compared to the ones present in Al₂O₃ and Pd/Al₂O₃. Therefore the catalyst with the highest
252 active acidity is γ - Al₂O₃ followed by Pd/Al₂O₃, Rh/Al₂O₃ and Ru/Al₂O₃.

253 Table 3: Total acidity, acidity retention and active acidity of γ -alumina, Rh/Al₂O₃, Ru/Al₂O₃ and
254 Pd/Al₂O₃.

	Total acidity^a (mmol NH₃/g cat.)	Acidity retention^b (%)	Active acidity (mmol NH₃/g cat.)
γ-alumina	1.51	100 (100°C) 92 (200°C) 92 (300°C)	1.51 (100°C) 1.39 (200°C) 1.39 (300°C)
Rh/Al₂O₃	1.34	100 (100 °C) 71 (200°C) 49 (300°C)	1.34 (100°C) 0.95 (200°C) 0.66 (300°C)
Ru/Al₂O₃	0.78	100 (100°C) 77 (200°C) 51 (300°C)	0.78 (100°C) 0.60 (200°C) 0.40 (300°C)
Pd/Al₂O₃	0.76	100 (100°C) 99 (200°C) 98 (300 °C)	0.76 (100°C) 0.75 (200°C) 0.74 (300°C)

255 **a)** Data obtained from NH₃-TPD **b)** Data obtained from DRIFT

256

257 **3.2. Screening experiments: effect of the type of catalyst**

258 **3.2.1 Effect of the catalyst, temperature and time on the oil and solid yield**

259 The main goal of this experimental set was to determine which catalyst performs best in the terms of
 260 high oil and low solid yield. For this purpose three analogous experimental sets for the Pd, Rh and Ru
 261 catalysts were subjected to surface response modelling. The experiments were performed randomly
 262 to minimize the systematic error. The results obtained for the oil and solid yield are summarized in
 263 Table 4.

264 **Table 4** Experimental design for screening experiments and oil and solid yields

Experiment	Oil Yield (%)	Solid Yield (%)	H/C	O/C	Mw	Ph*	Gu*	Ca*	Cr*	M-Gu*
Pd-1	86.1	12.8	1.19	0.21	444	2.6	4.2	1.1	5.8	3.8
Pd-2	57.1	6.2	1.18	0.1	305	2.8	3.3	0.7	5.3	3.7
Pd-3	38.2	60.3	1.24	0.26	538	2.3	3.7	0.3	0.0	3.4
Pd-4	78.5	7.5	1.15	0.16	404	2.0	2.9	1.7	4.3	2.8
Pd-5	81.7	2.8	1.21	0.14	323	2.5	3.4	2.0	5.2	3.4
Pd-6	85.4	2.4	1.19	0.17	332	1.9	2.8	2.0	3.9	2.6
Pd-7	81.6	2.9	1.21	0.18	340	2.2	3.1	2.0	4.6	3.0
Rh-1	83.0	16.5	1.22	0.22	556	2.0	3.4	1.1	4.6	3.1
Rh-2	58.9	5.7	1.18	0.1	187	2.0	2.6	0.6	4.3	2.9
Rh-3	38.4	56.4	1.25	0.26	561	3.4	5.3	0.3	0.0	5.0
Rh-4	74.0	5.2	1.15	0.16	296	1.7	2.5	1.1	3.6	2.4
Rh-5	81.0	4.8	1.21	0.14	344	1.4	2.0	1.3	2.9	1.9
Rh-6	83.9	4.0	1.2	0.16	388	1.3	1.9	1.7	2.8	1.8
Rh-7	76.6	5.0	1.2	0.16	420	1.4	2.0	1.5	2.9	1.9
Ru-1	91.8	10.1	1.23	0.18	688	2.4	4.0	1.3	5.2	3.5
Ru-2	60.7	5.0	1.19	0.09	359	2.5	2.7	0.4	4.4	0.0
Ru-3	37.0	61.9	1.25	0.26	721	2.1	3.4	0.3	4.7	3.1
Ru-4	83.9	8.2	1.17	0.17	497	1.5	2.3	1.7	3.2	2.1
Ru-5	90.0	5.1	1.21	0.19	490	1.6	4.5	2.4	6.7	4.4
Ru-6	84.2	3.3	1.21	0.19	522	1.3	3.9	2.1	5.5	1.7
Ru-7	86.2	3.2	1.21	0.19	487	2.0	3.2	1.9	4.3	2.8

265 **Pd:** Pd/Al₂O₃ was used as catalyst **Rh:** Rh/Al₂O₃ was used as catalyst **Ru:** Ru/Al₂O₃ was used as
 266 catalyst. The experimental conditions are given in Table 1. *: Phenol (Ph), cresol (Cr), guaiacol (Gu),
 267 methyl-guaiacol (M-Gu), catechol (Ca) and syringol (Sy) yields as %(weight) in the oil

268 Table S1, *Supplementary Information*, shows the results of the analysis of variance (ANOVA) of the
 269 fitted models for the oil and solids yields. The ANOVA results illustrate that none of the models are
 270 significant for a 90 % confidence interval. Nevertheless, the aim of this section is not to build

271 significant models but to evaluate the effect of the type of catalyst, temperature and reaction time in
 272 the response variables.

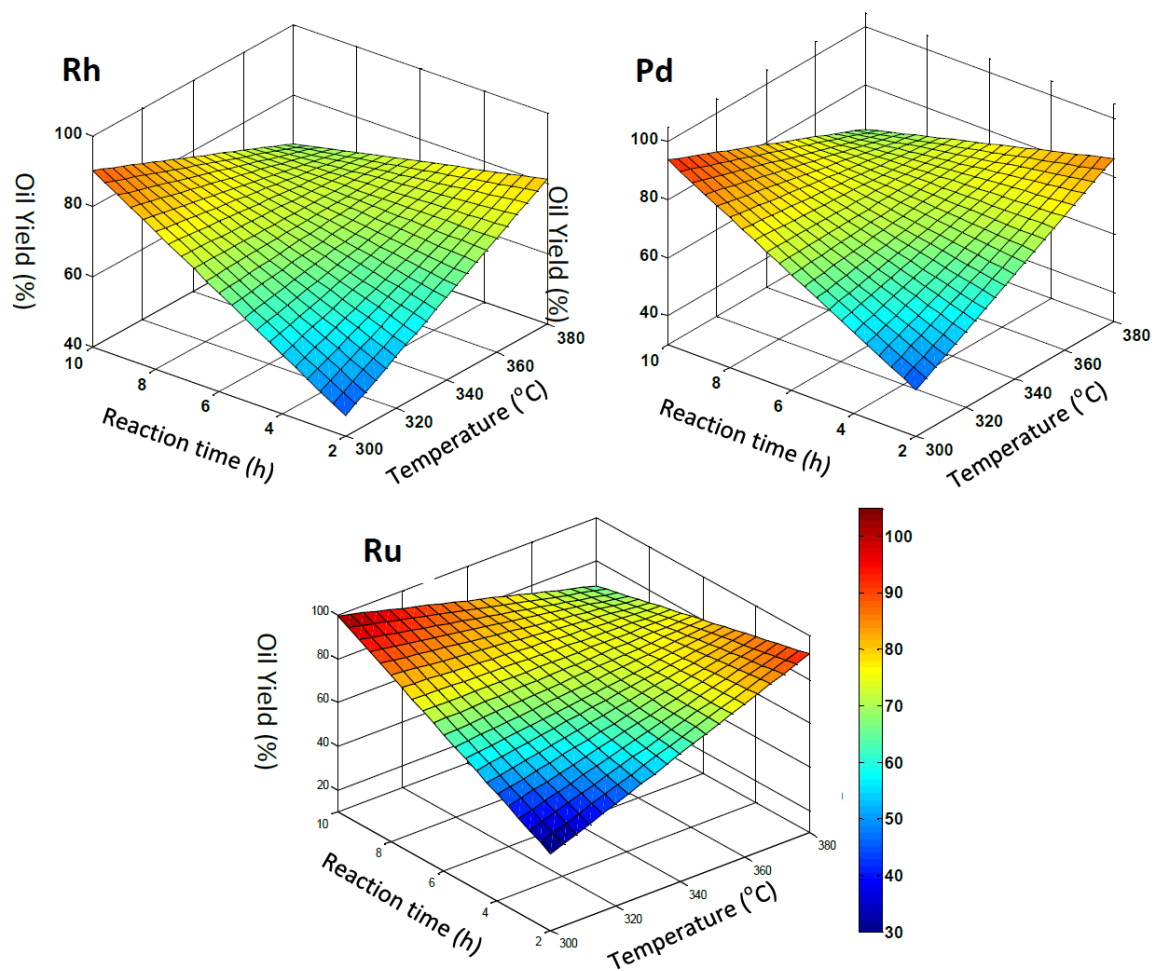
273 Figure 1 and Figure 2 show the surface response models for each catalyst system; the former
 274 describes the oil yields while the latter the solid yields. Note that the temperature and reaction time
 275 axes are in different position for the oil and solid yield. The fitted equations for the oil and char yield
 276 are presented in Table 5. From the results depicted one main conclusion is obtained: the Ru, Pd and
 277 Rh systems behave similarly for both the oil and solid yield, with regression coefficients that are of
 278 the same sign and comparable magnitude.

279 Table 5 Fitted equations for the oil and solid yield

System		Equation
Pd^a	Oil Yield (%)^d	Y = 72.66 + 2.83X₁ + 6.63X₂ - 17.33X₁X₂
Rh^b		Y = 70.83 + 2.88X₁ + 7.38X₂ - 14.93X₁X₂
Ru^c		Y = 76.25 + 3.95X₁ + 7.9X₂ - 19.5X₁X₂
Pd^a	Solid Yield (%)^e	Y = 13.56 - 14.85X₁ - 12.2X₂ + 11.55X₁X₂
Rh^b		Y = 13.94 - 15.5X₁ - 9.85X₂ + 10.1X₁X₂
Ru^c		Y = 13.83 - 14.7X₁ - 13.75X₂ + 12.15X₁X₂

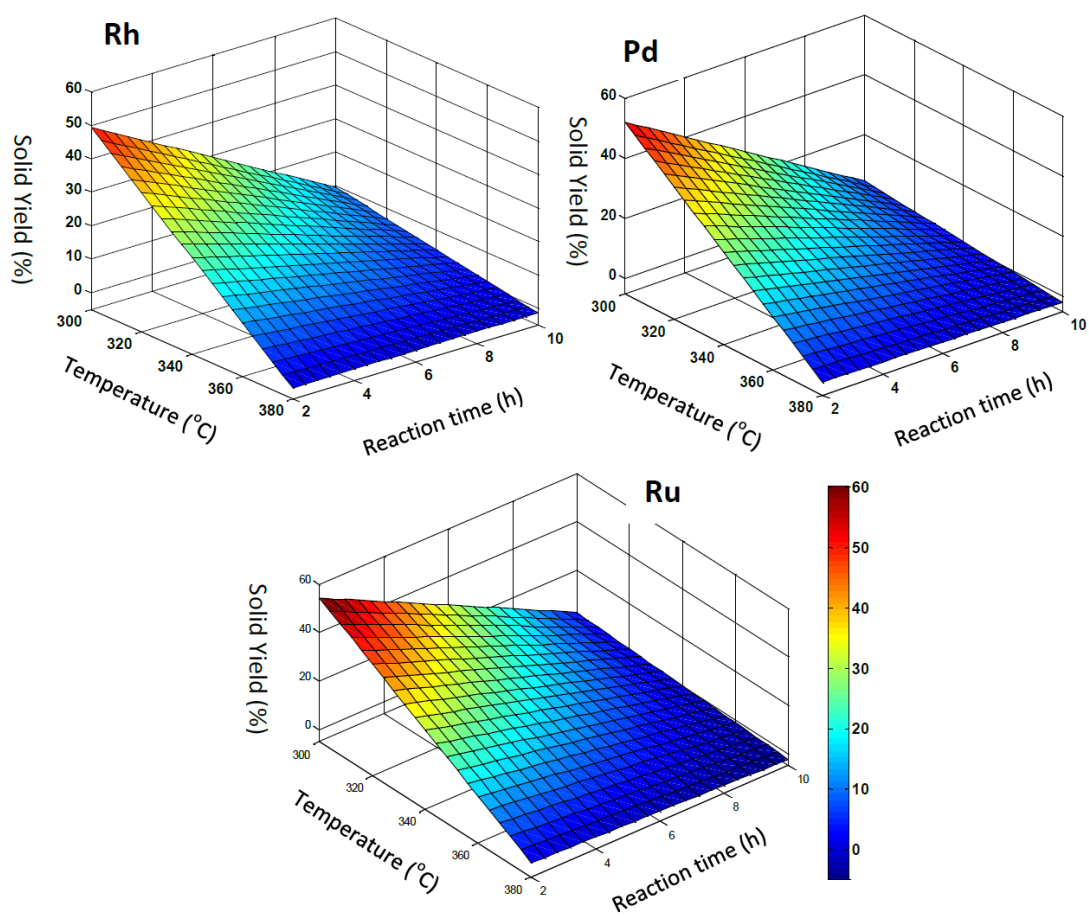
280 **Pd:** Pd/Al₂O₃ system **Rh:** Rh/Al₂O₃ system **Ru:** Ru/Al₂O₃ system **Oil Yield (%):** regression model built
 281 for the oil yield (%) **Solid Yield:** regression model built for the solid yield (%)

282 According to the fitted equations, high temperatures or long reaction times increase the oil and
 283 decreases the solid yield; while the sign of the cross-term coefficient suggests that the maximum is
 284 found out of the experimental space, toward the corners. This is confirmed by the analysis of the
 285 surface response models in Figure 1, which showed that the highest oil yields are found at low
 286 temperatures and long reaction times and/or at high temperatures and short reaction times. When
 287 comparing the oil yields it is clear that the Ru system gives the highest values, followed by Pd and Rh
 288 system. Lesser differences are seen in terms of solid yield, with the best results being obtained for
 289 the Pd catalyst, followed by the Ru and Rh. Therefore, Ru is selected as the best catalyst overall in
 290 terms of oil and solid yield. The behavior of this catalyst in the experimental space, together with the
 291 Al and NC system, will be quantitatively analyzed in Section 3.3.1.



293

294 Figure 1: Response surface models for the oil yields. **Rh:** Rh/Al₂O₃ catalyzed system, **Pd:** Pd/Al₂O₃295 catalyzed system , **Ru:** Ru/Al₂O₃ catalyzed system



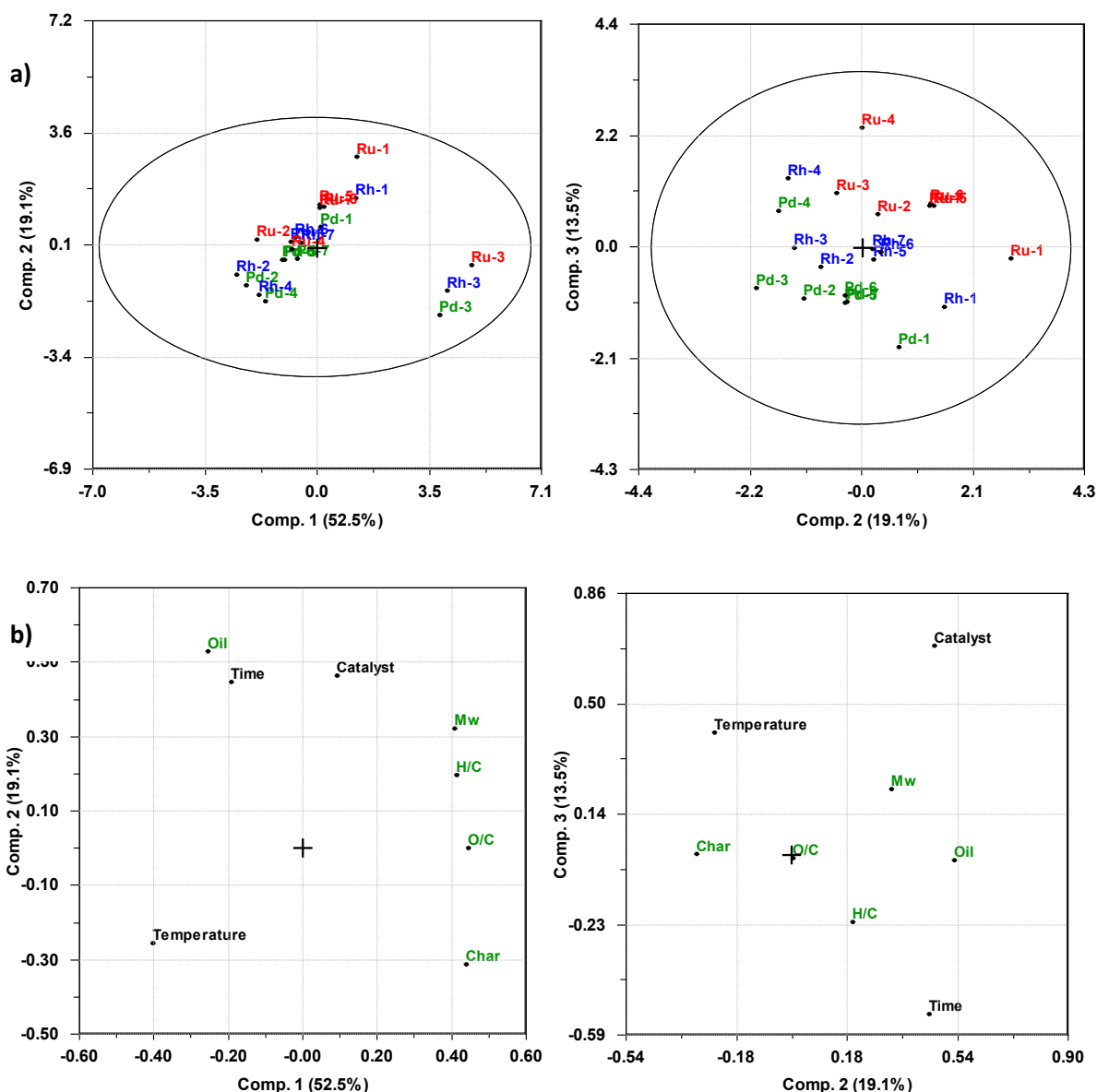
296

297 Figure 2: Response surface models for the solid yields. **Rh**: Rh/Al₂O₃ catalyzed system, **Pd**: Pd/Al₂O₃

298 catalyzed system , **Ru**: Ru/Al₂O₃ catalyzed system

299 **3.2.2 Effect of type of catalyst, temperature and reaction time in the quality of the oil (PCA)**

300 The aim of this section is mainly to establish the effect of the type of supported catalyst (Ru,Rh and
 301 Pd) on the quality of the oil, although correlations between time, temperature and oil quality will
 302 also be discussed. The values of the variables studied are summarized in Table 4. 85 % of the
 303 explained variance is described by three principal components (PCs). When analyzing the score plots
 304 (Figure 3a) it can be observed that the objects are somehow grouped together according to the type
 305 of catalyst (Ru in red, Rh in blue and Pd in green) and reaction conditions. Thus there is a correlation
 306 between the oil quality, oil and solid yield, the type of catalyst and the reaction conditions.



307

308

309 Figure 3: Score and loading plots for the quality of the oil. a) Score plots of the PCA analysis for the
 310 catalyst screening. Pd experiments in green, Rh experiments in blue, Ru experiments in red b)
 311 Loading plots of the PCA analysis for the catalyst screening. Factors describing the reaction

312 conditions in black, factors describing the oil yield (oil), solid yield (char) and quality of the oil (H/C,
313 O/C and M_w) in green. Coding for the response variables is given in Table 1.

314 When analyzing the loading plots (Figure 3b), some correlations between the design variables and
315 the oil quality variables can be observed. The most obvious observation is that the M_w is positively
316 correlated to the catalyst variable in all cases. This means that the Ru catalyst gives the oils with the
317 highest average molecular weight distributions followed by the Rh and Pd catalysts. Previous results
318 obtained in our group [19] suggest that the average molecular weight is dependent on the active
319 acidity of the alumina support (see Section 3.1), since lowering the active acidity resulted in an
320 increase in the average molecular weight within the oils. This correlation is therefore confirmed by
321 the data present in this study. M_w is negatively correlated to the temperature and reaction time on
322 PC1, which explains up to 52.5 %. Further analysis of the data in Table 4 confirms this correlation;
323 increasing the temperature and prolonging the reaction time resulted in oils with low molecular
324 weight. For a given reaction temperature, lower M_w values are obtained at longer reaction times.

325 A strong negative correlation is found between the temperature and the H/C ratio, while no or weak
326 correlations are found between the catalyst and the H/C ratio. When analyzing the data in Table 4
327 three trends can be identified: (i) at low temperatures the H/C ratio decreases with the reaction
328 time, (ii) at high temperatures the H/C ratio increases with the reaction time, and (iii) slightly higher
329 H/C ratios are obtained for the Ru system. In terms of O/C ratio, there is a clear negative correlation
330 between this variable and the temperature and reaction time, while no correlation is found between
331 the O/C ratio and the catalyst variable. This is confirmed when analyzing the raw data in Table 4,
332 illustrating that high temperatures and long reaction times are the most beneficial conditions in
333 terms of low O/C ratio. Hence the data shows two different behaviors in the elemental analysis of
334 the oils depending on the temperature level. At low temperature both the O/C and H/C ratios
335 decrease, while at high temperatures the O/C decrease and the H/C increases.

336 Another interesting result is the lack of correlation between the oil yield and the quality of the oil
337 (H/C ratio, O/C ratio and M_w value). This is confirmed by both the loading plots and the analysis of
338 the raw data. High H/C, O/C ratios and M_w values are obtained at low oil yields. Hence, the best
339 reaction conditions are found around the center points: high oil yields coupled with relatively low
340 M_w values and O/C ratios and relatively high H/C ratios.

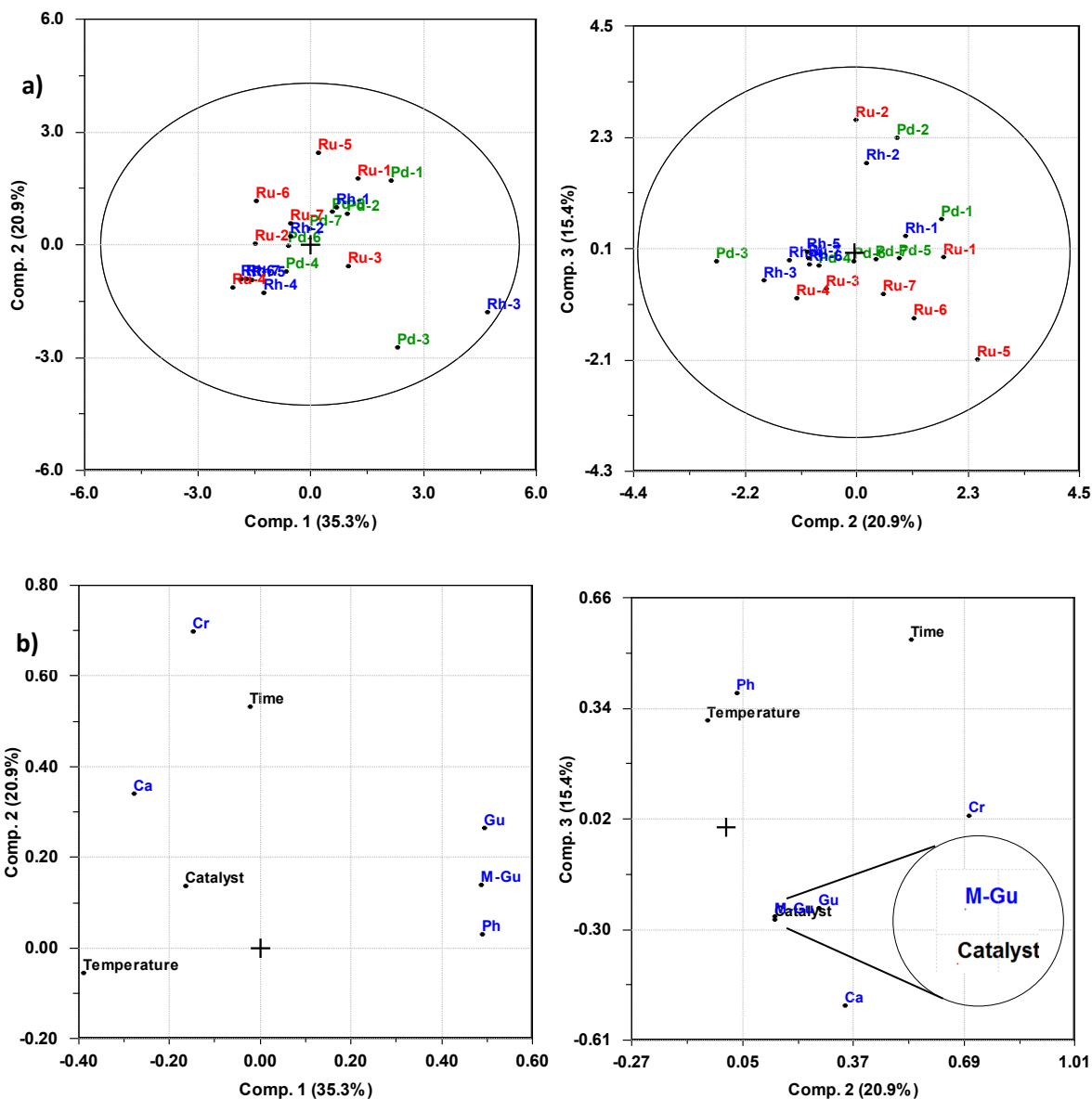
341

342 **3.2.3 Influence of the type of catalyst on the concentration of selected compounds**

343 The values submitted to PCA are given in Table 4. In the data analysis 71.55 % of the variance is
344 explained by three PCs. Figure 4 shows the score and loading plots. From the loading plots it can be
345 observed that those compounds bearing methoxy-groups, such as Gu and M-Gu, show only a strong
346 negative correlation with the temperature. Ca, a compound with two hydroxy-groups, is positively
347 correlated to the catalyst variable and non-correlated with the temperature and reaction time.
348 Compounds with only one hydroxy-group, such as Ph and Cr, are positively correlated with the
349 reaction time. The former, Ph, is also negatively correlated to the catalyst, and whilst the latter, Cr, is
350 positively correlated to the reaction time and catalyst variable.

351 These observations are in accordance with the behaviour of the elemental analysis of the oils
352 presented in Section 3.2.2. At low temperatures the H/C and O/C ratio decreases with time
353 suggesting that at this temperature level de-methoxylation and dehydration reactions of methoxy-
354 and hydroxyl- bearing compound are the prevailing reactions. However, at high temperatures, low
355 amount of methoxy- bearing compounds are found at low reaction times and the prevailing reaction
356 seems to be the alkylation of the monomers; which would justify both the increase of the H/C ratio
357 and the decrease of the O/C ratio.

358



359

360

361 Figure 4: Score and loading plots for the composition of the oil. a) Score plots of the PCA analysis for
 362 the catalyst screening. Pd experiments in green, Rh experiments in blue, Ru experiments in red b)
 363 Loading plots of the PCA analysis for the catalyst screening. Factors describing the reaction
 364 conditions in black, factors describing the concentration of certain components in blue. Coding for
 365 the response variables is given in Table 1

366 Previous work [29, 30] proposed the following mechanism. Lignin is initially depolymerized into
 367 primary products bearing methoxy groups such as syringol and different guaiacols. These react
 368 further accompanied with an increase in the degree of demethoxylation and deoxygenation of the
 369 different substituted species to yield catechols and thereafter phenols as stable products. Unlike this
 370 kinetic study, our experimental set is held at different temperatures. This might have distorted the
 371 actual correlations, but the loading plots still support the mechanism. At low temperatures, when the
 372 conversion rate is slow, Gu and M-Gu are in high concentrations. Ca is not correlated with any of the

373 reaction conditions, which could indicate that the compound is an intermediate. Finally, at long
 374 reaction times the concentration of Ph and Cr is the highest which suggest them as the end products.
 375 In terms of type of catalyst, Ru seems to favor the abundance of both catechol and cresol, while Pd
 376 seems to be the most suitable catalyst when oils with a high concentration in phenol are preferred.

377 3.3 Optimization experiments: Effect of the type of system

378 3.3.1 Influence of the type of system, temperature and reaction time on the oil and solid yields

379 In Section 3.2 several first order response surface models were built to analyze the effect of the type
 380 of catalyst, temperature and time, but none of them were statistically significant. In this section, the
 381 best catalyst in terms of oil and solid yield, Ru, is compared to additional reaction systems NC (non-
 382 catalyzed) and Al (γ -alumina catalyst) to evaluate which is the effect of the alumina support and the
 383 noble metal (Ru) in the reaction in a central composite design with a wider experimental basis for the
 384 modelling. The results obtained for the oil and solid yield are summarized in Table 6.

385 **Table 6:** Experimental design for optimization experiments and oil and solid yields

Experiment	Oil Yield (%)	Solid Yield (%)	H/C	O/C	Mw	Ph*	Gu*	Ca*	Cr*	M-Gu*
NC-1	64.8	31.7	1.13	0.2	431	1.9	3.3	1.5	4.2	2.8
NC-2	50.2	16.2	1.17	0.08	206	2.9	3.7	0.5	5.9	4.3
NC-3	32.1	57.5	1.17	0.24	553	1.7	3.4	0.6	3.9	2.7
NC-4	54.0	26.3	1.11	0.17	294	2.7	4.2	3.7	5.9	3.9
NC-5	58.2	22.4	1.19	0.18	346	1.7	2.5	2.0	3.6	2.4
NC-6	62.3	23.0	1.21	0.21	327	1.8	2.6	2.9	3.6	2.4
NC-7	64.2	16.5	1.21	0.2	339	2.1	3.0	2.8	4.3	2.8
NC-S1	41.4	21.3	1.1	0.15	95	2.8	2.4	0.5	4.2	3.5
NC-S2	31.0	63.6	1.17	0.29	928	2.1	3.7	0.8	0.0	3.2
NC-S3	13.5	83.4	1.29	0.33	548	2.2	3.3	0.4	5.1	3.0
NC-S4	63.2	16.6	1.11	0.16	258	2.4	3.0	1.4	4.7	3.0
Ru-1	91.8	10.1	1.23	0.18	688	2.4	4.0	1.3	5.2	3.5
Ru-2	60.7	5.0	1.19	0.09	359	2.5	2.7	0.4	4.4	0.0
Ru-3	37.0	61.9	1.25	0.26	721	2.1	3.4	0.3	4.7	3.1
Ru-4	83.9	8.2	1.17	0.17	497	1.5	2.3	1.7	3.2	2.1
Ru-5	90.0	5.1	1.21	0.19	490	1.6	4.5	2.4	6.7	4.4
Ru-6	84.2	3.3	1.21	0.19	522	1.3	3.9	2.1	5.5	1.7
Ru-7	86.2	3.2	1.21	0.19	487	2.0	3.2	1.9	4.3	2.8
Ru-S1	59.3	5.5	1.11	0.11	91	2.7	4.5	0.6	6.2	2.2
Ru-S2	45.5	48.3	1.27	0.4	2150	1.5	2.6	0.2	3.6	0.0
Ru-S3	30.8	67.6	1.17	0.27	2049	2.5	4.7	0.4	5.9	3.9
Ru-S4	79.8	3.3	1.18	0.16	468	2.8	5.5	2.0	6.7	4.3
Al-1	84.8	16.1	1.18	0.23	276	1.2	2.3	1.2	2.8	2.3
Al-2	48.2	17.3	1.2	0.1	178	2.4	2.7	0.6	4.9	4.6

Al-3	36.8	61.8	1.22	0.27	318	2.3	4.2	0.5	0.0	4.0
Al-4	57.4	24.5	1.16	0.21	211	1.6	2.4	3.4	3.4	2.6
Al-5	63.1	22.0	1.2	0.21	215	1.4	2.2	3.1	3.2	2.3
Al-6	58.7	25.7	1.18	0.17	225	2.0	2.9	3.0	4.3	3.0
Al-7	66.5	17.1	1.19	0.19	210	2.5	3.6	2.9	5.5	3.8
Al-S1	43.3	21.0	1.12	0.12	108	2.8	3.0	0.5	5.6	4.5
Al-S2	49.8	52.1	1.19	0.25	1360	1.9	3.4	0.5	0.0	3.5
Al-S3	13.3	82.8	1.36	0.32	826	2.1	3.3	0.3	5.5	3.3
Al-S4	65.4	11.1	1.19	0.16	347	2.4	3.0	1.4	5.1	3.3

386 **NC:** non-catalysed experiments **Ru:** Ru/Al₂O₃ was used as catalyst **Al:** γ-Al₂O₃ was used as catalyst. **S:**
387 refers to the axial points were α=1.41. The experimental conditions are given in Table 2. *: Phenol
388 (Ph), cresol (Cr), guaiacol (Gu), methyl-guaiacol (M-Gu), catechol (Ca) and syringol (Sy) yields as
389 %(weight) in the oil

390 The analysis of the variance (ANOVA) (Table S2, *Supplementary Information*), shows that all the
391 models are significant for a confidence level of 90 %, which allows a quantitative analysis of the
392 results. Table 7 displays the second order regression models for the oil and solid yield. The surface
393 response models for the oil and solid yield are presented in Figures 5 and 6 respectively.

394 Ru gives higher oil and lower solid yields in the experimental space. The maximum oil and minimum
395 solid yield is found around the center of the experimental space, and more precisely toward the area
396 of low temperatures and long reaction times. This model differs from the one obtained in Section
397 3.2.1 where the maximum was not found within the experimental space. Hence, quadratic terms are
398 important to provide significant models of the systems.

399 **Table 7:** Regression second order models for the oil yield and solid yield

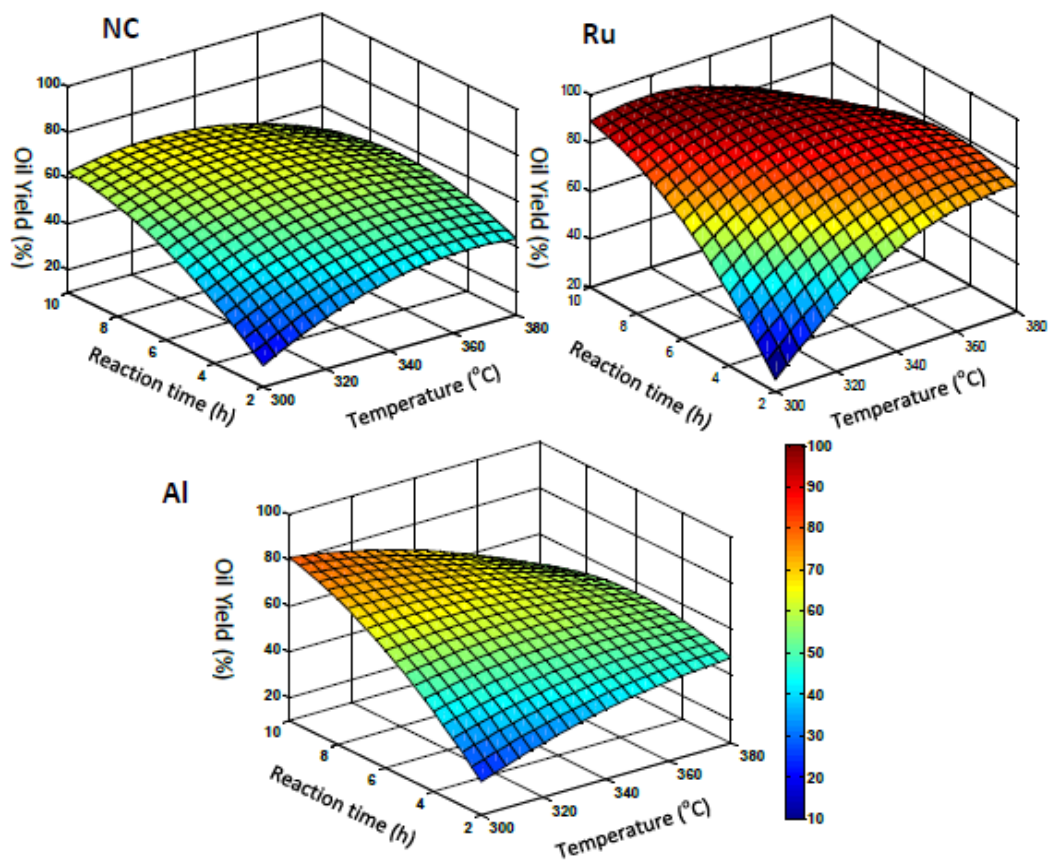
System		Equation
NC ^a	Oil Yield (%) ^d	$Y = 61.56 + 2.75X_1 + 12.40X_2 - 9.43X_1^2 - 8.36X_2^2 - 9.13X_1X_2$
Ru ^b		$Y = 86.79 + 4.41X_1 + 12.61X_2 - 19.5X_1^2 - 13.57X_2^2 - 12.12X_1X_2$
Al ^c		$Y = 62.76 - 3.15X_1 + 14.06X_2 - 4.64X_1^2 - 8.25X_2^2 - 14.3X_1X_2$
NC ^a	Solid Yield (%) ^e	$Y = 20.64 - 13.32X_1 - 16.30X_2 + 7.58X_1^2 + 11.36X_2^2 - 3.93X_1X_2$
Ru ^b		$Y = 3.87 - 14.92X_1 - 18.24X_2 + 12.15X_1^2 + 9.05X_2^2 + 12.32X_1X_2$
Al ^c		$Y = 21.6 - 10.01X_1 - 19.29X_2 + 4.52X_1^2 + 9.72X_2^2 + 9.63X_1X_2$

400 **NC:** non-catalysed reaction system **Ru:** Ru/Al₂O₃ was used as catalyst **Al:** γ-Al₂O₃ was used as catalyst
401 **Oil Yield (%):** regression model built for the oil yield (%) **Solid Yield:** regression model built for the
402 solid yield (%)

403 The NC systems give significantly lower oil yields than the Ru. However, the regression coefficients
404 are of the same sign and the shape of the response surface is similar, and the maximum oil yield is
405 found around the same area. On the other hand the oil yield maximum for the Al system is not found
406 within the experimental space. This is because unlike Ru and NC, the Al system is negatively

407 correlated to the temperature, shifting the maximum towards the area of low temperatures and long
408 reaction times.

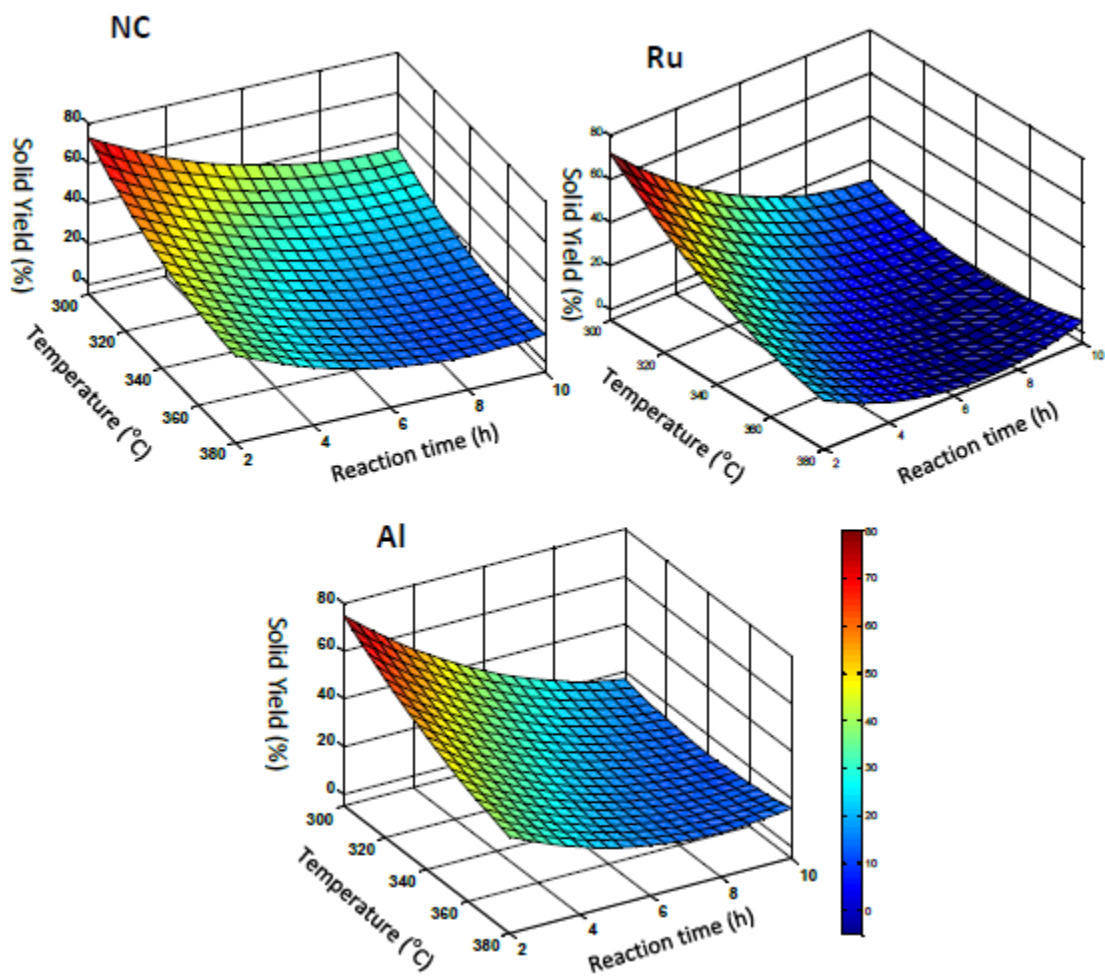
409 The analysis of the solid yields (Figure 6 and Table 7), confirms the conclusions described above.
410 Note that the axes regarding the temperature and reaction time are opposite the previous plot. NC
411 and Ru systems behave analogously, although considerably lower solid values are obtained for the
412 Ru system. However in the case of the Al system, the lowest solid yields are obtained in the areas of
413 low temperatures and long reaction times. This confirms that the presence of γ -alumina increases
414 the oil yield at low temperatures, while the presence of the noble metal Ru supported on the
415 alumina increases the oil yield in the experimental space. This is in accordance with our previous
416 results [19], suggesting that the alumina support can catalyze both the de-polymerization and re-
417 polymerization reactions. Hence at low temperatures, where de-polymerization is favored, the oil
418 yield for the Al systems increases, and while at high temperatures this effect is neutralized by the
419 increase of the re-polymerization rate. It is noteworthy that at 380°C the oil yield is slightly higher for
420 the Al system (57.4 %) than that of the NC system (54.0 %) when the reaction time is 2 h, while the
421 oil yield is slightly higher for the NC system (50.2 %) than for the Al system (48.2 %) when the
422 reaction time is 10 h.
423



424

425 Figure 5: Response surface models for the oil yield. NC: non-catalyzed system, Ru: Ru/Al₂O₃ catalyzed

426 system, Al: γ-Al₂O₃ catalyzed system



427

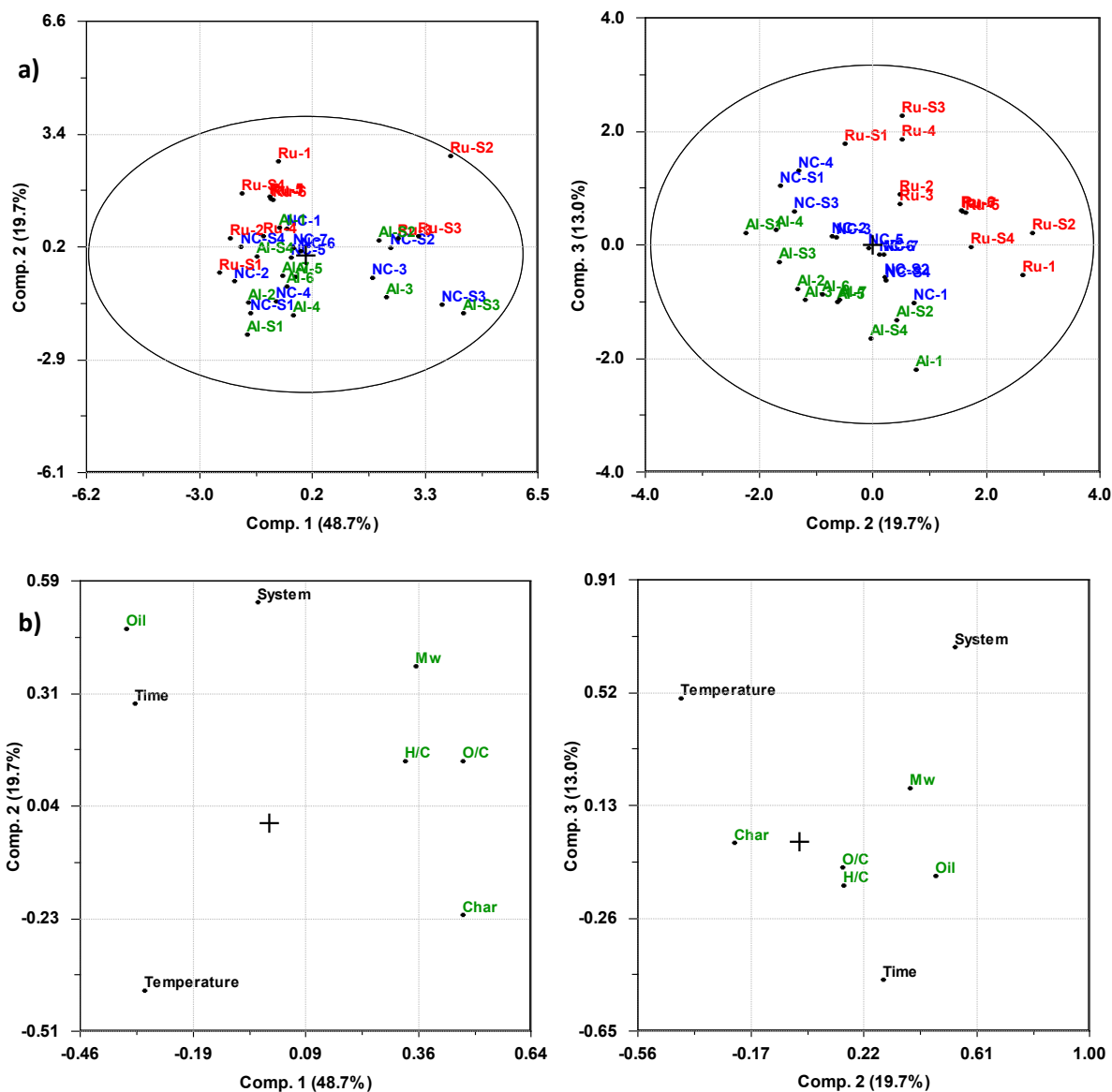
428 Figure 6: Response surface models for the solid yield. NC: non-catalyzed system, Ru: Ru/Al₂O₃

429 catalyzed system, Al: γ-Al₂O₃ catalyzed system

430

431 **3.3.2 Effect of type of system, temperature and reaction time in the quality of the oil**

432 The system variable, accompanied by the temperature, reaction time, oil yield, solid yield and the oil-
 433 quality responses are submitted to an exploratory PCA. Table 6 describes the values of the different
 434 responses. 81.5 % of the variance is explained by three PC. The score plots depicted in Figure 7.a
 435 show that the objects are group in terms of system and reaction conditions, although this patterns is
 436 less clear than in Section 3.2.2. On the other hand, the loading plots in Figure 7.b significantly
 437 resemble the corresponding plots in Section 3.2.2.



440 Figure 7: Score plots and loading plots for composition of the oil. a) Score plots of the PCA analysis
 441 for the catalyst optimization. Al experiments in green, NC experiments in blue, Ru experiments in red
 442 b) Loading plots of the PCA analysis for the optimization experiments. Factors describing the reaction
 443 conditions in black, factors describing the oil yield (oil), solid yield (char) and quality of the oil (H/C,
 444 O/C and M_w) in green. The coding for the response variables is given in Table 2.

445 The most obvious correlation is again the one between the system variables and the M_w . This means
446 that the Ru systems produce oils with higher average molecular weights, while the lowest M_w values
447 are obtained for the Al. In the absence of catalyst, the values of M_w are lower than the ones for the
448 Ru but higher than the ones for the Al systems. This phenomenon could be due the fact that the Ru
449 catalyst, the Ru active phase, can stabilize high M_w oligomers through hydrodeoxygenation [31] and
450 alkylation reactions[32], while in the case of the Al and NC systems these compounds are re-
451 polymerized into solid. The lowest values of M_w obtained in the Al system could be due to the high
452 active acidity of the γ -alumina, a phenomenon already observed in Section 3.2.2. The loading plots
453 and the raw data in Figure 7.b suggest that the temperature and reaction time are negatively
454 correlated to the M_w , and support that high temperatures and long reaction times favor lignin de-
455 polymerization.

456 The behavior of the H/C ratio with respect to the temperature and reaction time is in accordance
457 with the results observed in Section 3.2.2. At low temperatures the H/C ratio decreases with the
458 reaction time while at high temperatures this values increases. From the loading plot (Figure 7a) no
459 or weak correlations are found between the system, reaction time and H/C variables. However, the
460 data in Table 6 clearly shows that the Ru (+1) system gives higher H/C ratio oils, followed by the Al (-
461 1) and the NC (0) system.

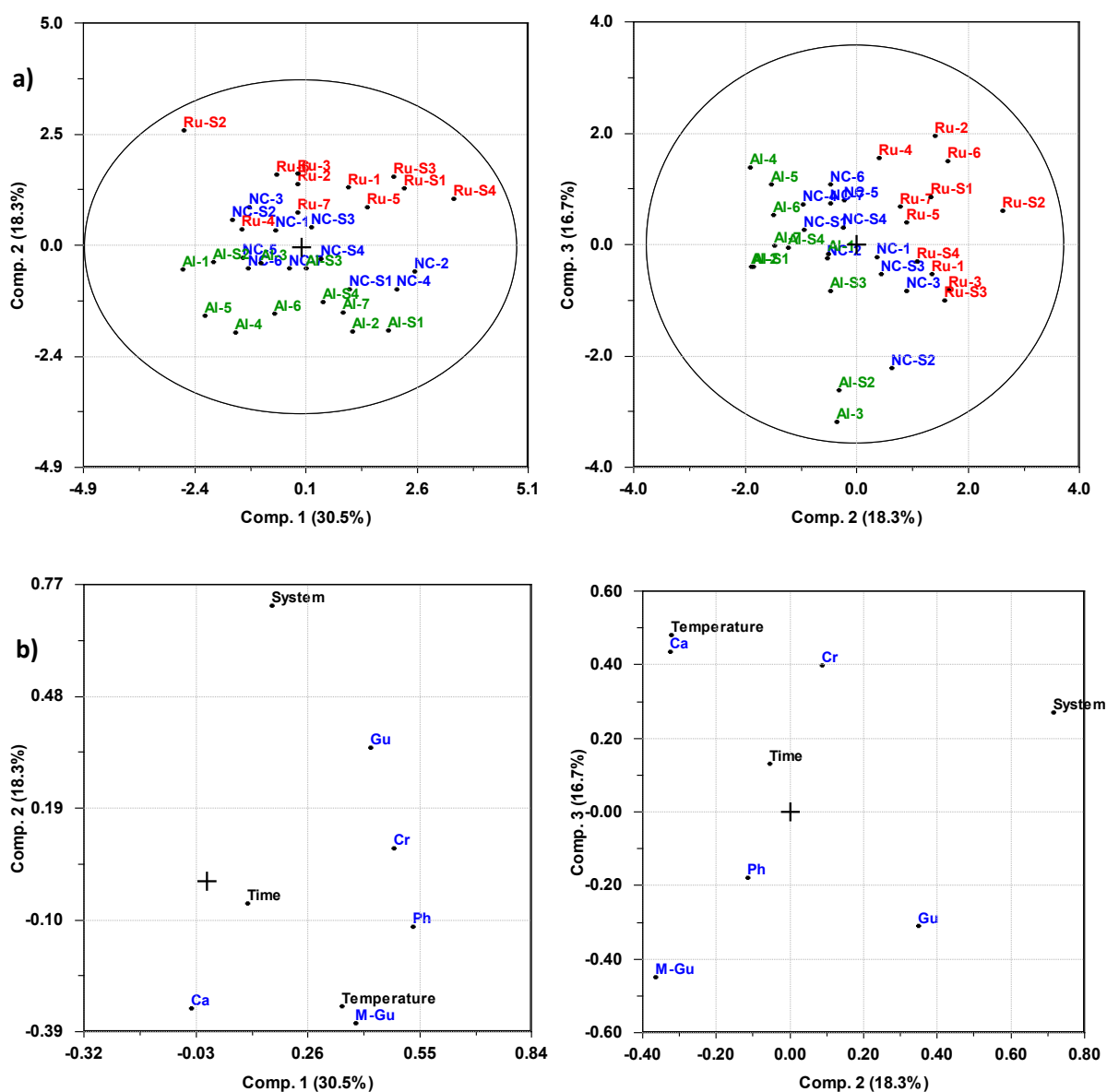
462 The O/C ratio is not considerably influenced by the type of system. Temperature is again negatively
463 correlated to the O/C ratio, while the correlation with the reaction time is not so clear when
464 analyzing the score plots. Nevertheless, the raw data again indicates that the higher the temperature
465 and the longer the reaction time, the lower the O/C ratio.

466 As in Section 3.2.2 there is a lack of correlation between the oil yield and the variables selected to
467 evaluate the quality of the oil. Some other aspects are also confirmed: (i) the active acidity of the
468 catalysts decreases the M_w value, (ii) the H/C ratio is negatively correlated to the temperature, (iii)
469 the O/C ratio is negatively correlated to temperature and reaction time, and (iv) the best results are
470 found in the center of the experimental space. An additional observation is that the presence of the
471 noble metal is positive for the H/C ratio, which can be explained by catalysis of the hydrogenation of
472 the end products, as expected.

473 3.3.3 Analysis of the concentration of main compounds

474 Table 6 describes the values of the variables submitted to exploratory PCA. As in Section 3.2.3, five
475 main components were selected (Ph, Gu, Ca, Cr, MGu). The first three PCs describe only 65.5 % of the
476 variance. From the analysis of the score plot in Figure 8.a, it can be observed that the objects are
477 mainly grouped by the type of the system. The loading plots in Figure 8.b show that the variance is

478 largely explained by the system variable, especially on PC2. All this indicates that there are significant
 479 differences on the kinetic or mechanistic pathways between the systems. When analyzing the
 480 correlations for each compound no clear patterns are observed. Each component is differently
 481 correlated to the temperature, reaction time and system variable depending on the PC. This shows
 482 that the significant difference in the reaction mechanisms prevent clear conclusions about how the
 483 experimental variables studied affect the composition of the oil using this multivariate approach.



484

485

486 Figure 8: Score and loading plots of the composition of the oil. a) Score plots of the PCA analysis for
 487 the optimization experiments. Al experiments in green, NC experiments in blue, Ru experiments in
 488 red b) Loading plots of the PCA analysis for the optimization experiments. Factors describing the
 489 reaction conditions in black, factors describing the concentration of certain components in blue. The
 490 coding for the response variables is given in Table 2.

491

492 **3.4 Recycling of the catalyst**

493 The inorganic ash content of the lignin is 1.5 wt%. The average value of the recovered organic solids
 494 (char) and lignin-derived inorganic ashes for the Ru system, at 340°C and 6 hours, is 2.7 wt%. This
 495 means that the solids recovered after the reaction mainly comprises the catalyst. After the thermal
 496 treatment the organic matter was eliminated, giving a recovered catalyst with a small amount of
 497 inorganic impurities derived from the lignin (ashes).

498 The catalyst was recycled twice, and its activity was evaluated in terms of oil and solid yields. For the
 499 first cycle three replicates were made (Ru-A1, Ru-A2 and Ru-A3), while two replicates were carried
 500 out for the second recycling cycle (Ru-B1 and Ru-B2).

501 Table 11 shows the results obtained for both cycles. Surprisingly, the average values show that the
 502 oil yield is maintained or increased upon recycling. The solid yield is comparable for all the reaction
 503 cycles. The variation could be assigned to experimental uncertainty during the work-up procedure.

504 Table 11: Oil yield, H/C and O/C ration of the oil and solid yield for the recycling experiments

Experiment Name	Oil Yield (% on lignin)	Average Oil Yield (% on lignin)	H/C	O/C	Solid Yield (% on lignin)	Average Solid Yield (% on lignin)
Ru-5	90.0	86.8	1.21	0.19	5.1	3.9
Ru-6	84.2		1.21	0.19	3.3	
Ru-7	86.2		1.21	0.19	3.2	
Ru-A1	84.9	86.8	1.20	0.19	2.7	2.6
Ru-A2	88.7		1.18	0.18	2.5	
Ru-A3	86.7		1.16	0.18	2.5	
Ru-B1	88.9	91.6	1.22	0.20	4.7	4.6
Ru-B2	94.2		1.22	0.19	4.6	

505 **A:** refers to the replicates for first recycling cycle **B:** refers to the replicates for the second recycling
 506 cycle. Conditions: 340°C and 6 hours

507 Overall, the results show no deactivation of the catalyst in terms of oil and solid yield. The H/C and
 508 O/C ratio of the oils depicted in Table 11 confirm that there is no catalyst deactivation. The H/C ratios
 509 decrease slightly for some experiments in the first recycling cycle, but the results are comparable or
 510 higher for the second cycle. This means that the differences can be understood as a function of
 511 uncertainties during the work-up and/or the analytic procedures. The O/C ratio is also maintained
 512 within acceptable uncertainty limits.

513

514 4. Conclusion

515 Lignin from Norway spruce was successfully converted into aromatic based oil in the presence of
516 several noble metal catalysts supported in alumina in a formic acid water media. Oils were produced
517 over a range of reaction temperatures (283-397°C) and reaction times (2-10 h). Response surface
518 methodology (RSM) has been proven to be a successful tool to build significant models for the oil and
519 solid yield within the studied experimental space. Principal component analysis (PCA) is proven to be
520 a successful tool to evaluate the effect of the reaction variables on the oil quality and composition,
521 and to extract qualitative data on the reaction mechanism. The recycling of the catalyst shows that
522 the Ru catalyst fully retains its activity in two separate recycling tests.

523 This systematic approach improved the quantitative understanding of the process and successfully
524 confirmed features previously noted from less extensive investigations [19]. For the catalysts, both
525 the noble metal and the γ -alumina are active in the LtL process. The former increases the oil yield
526 while decreasing the solid yield. The latter is active in the lignin de-polymerization and in the re-
527 polymerization of the lignin monomers, and therefore increases the oil yield at low temperatures,
528 where re-polymerization is not favored. Among the noble metals studied Ru gives the highest oil
529 yield in the whole experimental space. A strong dependency between the active acidity of the
530 alumina support and the M_w of the oil has been also confirmed.

531 No correlations between the oil yield and the quality of the oil has been found. The oil yield is
532 strongly dependent on the presence of the catalyst, temperature and reaction time; while the oil
533 quality is mainly dependent on the temperature and reaction time. Therefore, the optimum reaction
534 conditions were found to be around 340°C and 6 h; where nearly complete conversion of lignin into
535 oil is achieved while still having high H/C ratios coupled with low O/C ratios and M_w values.

536 The study of the composition of the oil confirms that the reaction mechanism differs between the
537 supported catalyst (Ru/Al₂O₃, Pd/Al₂O₃ and Rh/Al₂O₃) system, the γ -Al₂O₃ system and the non-
538 catalyzed system. In the supported catalyst systems, the reaction comprises several steps. It starts
539 with the de-polymerization of the lignin; followed by de-methoxylation, dehydration and alkylation
540 of the monomers. At low temperatures de-methoxylation and dehydration reactions are
541 predominant for the reaction times studied, while at high temperatures these reactions take place at
542 short reaction times, followed by alkylation reactions. Thus, the final products obtained depend on
543 the reaction temperature: at high temperature alkylated compounds such as cresol are favored,
544 while at low temperatures non-alkylated compounds, such as phenol, are more abundant.

545 In an overall perspective, the results show the potential for improving the yields of oil by the use of
546 catalysts which are easily recovered, and suggest a good potential for tuning the oil composition to

547 specific compositions depending on the requirements for the product. Such processing of lignin
548 residues to phenol-type product compositions could be a complementary process to the
549 carbohydrate conversion in the utilization of lignocellulosic biomass in a bio-based refinery.

550 **5. Acknowledgement**

551 Some of this work has been performed as a part of the LignoRef project (“Lignocellulosics as a basis
552 for second generation biofuels and the future biorefinery”). We gratefully acknowledge The Research
553 Council of Norway (grant no. 190965/S60), Statoil ASA, Borregaard Industries Ltd., Allskog BA, Cambi
554 AS, Xynergo AS, Hafslund ASA and Weyland AS for financial support. The authors would also like to
555 thank I. J. Fjellanger for assisting with elemental analysis, Dr. Egil Nodland and Prof Bjørn Grung for
556 their assistance on RSM and PCA, and the Technical College of Bergen for supplying lignin.

557

- 558 [1] K.D. Maher, D.C. Bressler, Pyrolysis of triglyceride materials for the production of renewable fuels
559 and chemicals, *Bioresource Technology*, 98 (2007) 2351-2368.
- 560 [2] C.M. Sastre, Y. González-Arechavala, A.M. Santos, Global warming and energy yield evaluation of
561 Spanish wheat straw electricity generation – A LCA that takes into account parameter uncertainty
562 and variability, *Applied Energy*, 154 (2015) 900-911.
- 563 [3] B. Kamm, M. Kamm, *Biorefinery-Systems*, Chemical and Biochemical Engineering Quarterly, 18
564 (2004) 1-6.
- 565 [4] J. Zakzeski, P.C.A. Bruijninx, A.L. Jongerius, B.M. Weckhuysen, The Catalytic Valorization of Lignin
566 for the Production of Renewable Chemicals, *Chemical Reviews*, 110 (2010) 3552-3599.
- 567 [5] M. Kleinert, J.R. Gasson, T. Barth, Optimizing solvolysis conditions for integrated depolymerisation
568 and hydrodeoxygenation of lignin to produce liquid biofuel, *Journal of Analytical and Applied
569 Pyrolysis*, 85 (2009) 108-117.
- 570 [6] A. Limayem, S.C. Ricke, Lignocellulosic biomass for bioethanol production: Current perspectives,
571 potential issues and future prospects, *Progress in Energy and Combustion Science*, 38 (2012) 449-
572 467.
- 573 [7] H. Chen, X. Fu, Industrial technologies for bioethanol production from lignocellulosic biomass,
574 *Renewable and Sustainable Energy Reviews*, 57 (2016) 468-478.
- 575 [8] M.O.S. Dias, T.L. Junqueira, C.E.V. Rossell, R. Maciel Filho, A. Bonomi, Evaluation of process
576 configurations for second generation integrated with first generation bioethanol production from
577 sugarcane, *Fuel Processing Technology*, 109 (2013) 84-89.
- 578 [9] R. Gonzalez, J. Daystar, M. Jett, T. Treasure, H. Jameel, R. Venditti, R. Phillips, Economics of
579 cellulosic ethanol production in a thermochemical pathway for softwood, hardwood, corn stover and
580 switchgrass, *Fuel Processing Technology*, 94 (2012) 113-122.
- 581 [10] H.L. Chum, R.P. Overend, Biomass and renewable fuels, *Fuel Processing Technology*, 71 (2001)
582 187-195.
- 583 [11] C. Peng, G. Zhang, J. Yue, G. Xu, Pyrolysis of lignin for phenols with alkaline additive, *Fuel
584 Processing Technology*, 124 (2014) 212-221.
- 585 [12] A.L. Jongerius, P.C.A. Bruijninx, B.M. Weckhuysen, Liquid-phase reforming and
586 hydrodeoxygenation as a two-step route to aromatics from lignin, *Green Chemistry*, 15 (2013) 3049-
587 3056.
- 588 [13] Q. Bu, H. Lei, A.H. Zacher, L. Wang, S. Ren, J. Liang, Y. Wei, Y. Liu, J. Tang, Q. Zhang, R. Ruan, A
589 review of catalytic hydrodeoxygenation of lignin-derived phenols from biomass pyrolysis,
590 *Bioresource Technology*, 124 (2012) 470-477.

591 [14] B. Li, W. Lv, Q. Zhang, T. Wang, L. Ma, Pyrolysis and catalytic pyrolysis of industrial lignins by TG-
592 FTIR: Kinetics and products, *Journal of Analytical and Applied Pyrolysis*, 108 (2014) 295-300.

593 [15] M. Kleinert, T. Barth, Towards a Lignocellulosic Biorefinery: Direct One-Step Conversion of Lignin
594 to Hydrogen-Enriched Biofuel, *Energy & Fuels*, 22 (2008) 1371-1379.

595 [16] B. Holmelid, M. Kleinert, T. Barth, Reactivity and reaction pathways in thermochemical
596 treatment of selected lignin-like model compounds under hydrogen rich conditions, *Journal of*
597 *Analytical and Applied Pyrolysis*, 98 (2012) 37-44.

598 [17] F. Ates, N. Erginel, Optimization of bio-oil production using response surface methodology and
599 formation of polycyclic aromatic hydrocarbons (PAHs) at elevated pressures, *Fuel Processing*
600 *Technology*, 142 (2016) 279-286.

601 [18] L. Liguori, T. Barth, Palladium-Nafion SAC-13 catalysed depolymerisation of lignin to phenols in
602 formic acid and water, *Journal of Analytical and Applied Pyrolysis*, 92 (2011) 477-484.

603 [19] M. Oregui Bengoechea, A. Hertzberg, N. Miletić, P.L. Arias, T. Barth, Simultaneous catalytic de-
604 polymerization and hydrodeoxygenation of lignin in water/formic acid media with Rh/Al₂O₃,
605 Ru/Al₂O₃ and Pd/Al₂O₃ as bifunctional catalysts, *Journal of Analytical and Applied Pyrolysis*, 113
606 (2015) 713-722.

607 [20] S. Focardi, S. Ristori, S. Mazzuoli, A. Tognazzi, D. Leach-Scampavia, D.G. Castner, C. Rossi, ToF-
608 SIMS and PCA studies of Seggianese olives and olive oil, *Colloids and Surfaces A: Physicochemical and*
609 *Engineering Aspects*, 279 (2006) 225-232.

610 [21] T.-A. Ngo, J. Kim, S.-S. Kim, Characteristics of palm bark pyrolysis experiment oriented by central
611 composite rotatable design, *Energy*, 66 (2014) 7-12.

612 [22] H.A. Oramahi, Wahdina, F. Diba, Nurhaida, T. Yoshimura, Optimization of Production of
613 Lignocellulosic Biomass Bio-oil from Oil Palm Trunk, *Procedia Environmental Sciences*, 28 (2015) 769-
614 777.

615 [23] N. Smichi, Y. Messaoudi, A. Gelicus, K. Allaf, M. Gargouri, Optimization of DIC technology as a
616 pretreatment stage for enzymatic saccharification of *Retama raetam*, *Fuel Processing Technology*,
617 138 (2015) 344-354.

618 [24] H.V. Lee, R. Yunus, J.C. Juan, Y.H. Taufiq-Yap, Process optimization design for jatropha-based
619 biodiesel production using response surface methodology, *Fuel Processing Technology*, 92 (2011)
620 2420-2428.

621 [25] B.H. Hameed, L.F. Lai, L.H. Chin, Production of biodiesel from palm oil (*Elaeis guineensis*) using
622 heterogeneous catalyst: An optimized process, *Fuel Processing Technology*, 90 (2009) 606-610.

623 [26] R. Fahmi, A.V. Bridgwater, I. Donnison, N. Yates, J.M. Jones, The effect of lignin and inorganic
624 species in biomass on pyrolysis oil yields, quality and stability, *Fuel*, 87 (2008) 1230-1240.

625 [27] K.M. Sharif, M.M. Rahman, J. Azmir, A. Mohamed, M.H.A. Jahurul, F. Sahena, I.S.M. Zaidul,
626 Experimental design of supercritical fluid extraction – A review, *Journal of Food Engineering*, 124
627 (2014) 105-116.

628 [28] M. Tamura, H. Nishibayashi, M. Ogura, Y. Uematsu, T. Itakura, J.F. Mangin, J. Régis, S. Ikuta, K.
629 Yoshimitsu, T. Suzuki, C. Niki, Y. Muragaki, H. Iseki, MRI Based Sulcal Pattern Analysis for Diagnosis
630 and Clinical Application in Neurosurgery, in: T. Dohi, H. Liao (Eds.) *Computer Aided Surgery: 7th Asian*
631 *Conference on Computer Aided Surgery*, Bangkok, Thailand, August 2011, *Proceedings*, Springer
632 Japan, Tokyo, 2012, pp. 135-143.

633 [29] J.R. Gasson, D. Forchheim, T. Sutter, U. Hornung, A. Kruse, T. Barth, Modeling the Lignin
634 Degradation Kinetics in an Ethanol/Formic Acid Solvolysis Approach. Part 1. Kinetic Model
635 Development, *Industrial & Engineering Chemistry Research*, 51 (2012) 10595-10606.

636 [30] D. Forchheim, J.R. Gasson, U. Hornung, A. Kruse, T. Barth, Modeling the Lignin Degradation
637 Kinetics in a Ethanol/Formic Acid Solvolysis Approach. Part 2. Validation and Transfer to Variable
638 Conditions, *Industrial & Engineering Chemistry Research*, 51 (2012) 15053-15063.

639 [31] X. Huang, T.I. Korányi, M.D. Boot, E.J.M. Hensen, Catalytic Depolymerization of Lignin in
640 Supercritical Ethanol, *ChemSusChem*, 7 (2014) 2276-2288.

641 [32] R. Shu, J. Long, Y. Xu, L. Ma, Q. Zhang, T. Wang, C. Wang, Z. Yuan, Q. Wu, Investigation on the
642 structural effect of lignin during the hydrogenolysis process, *Bioresource Technology*, 200 (2016) 14-
643 22.

644

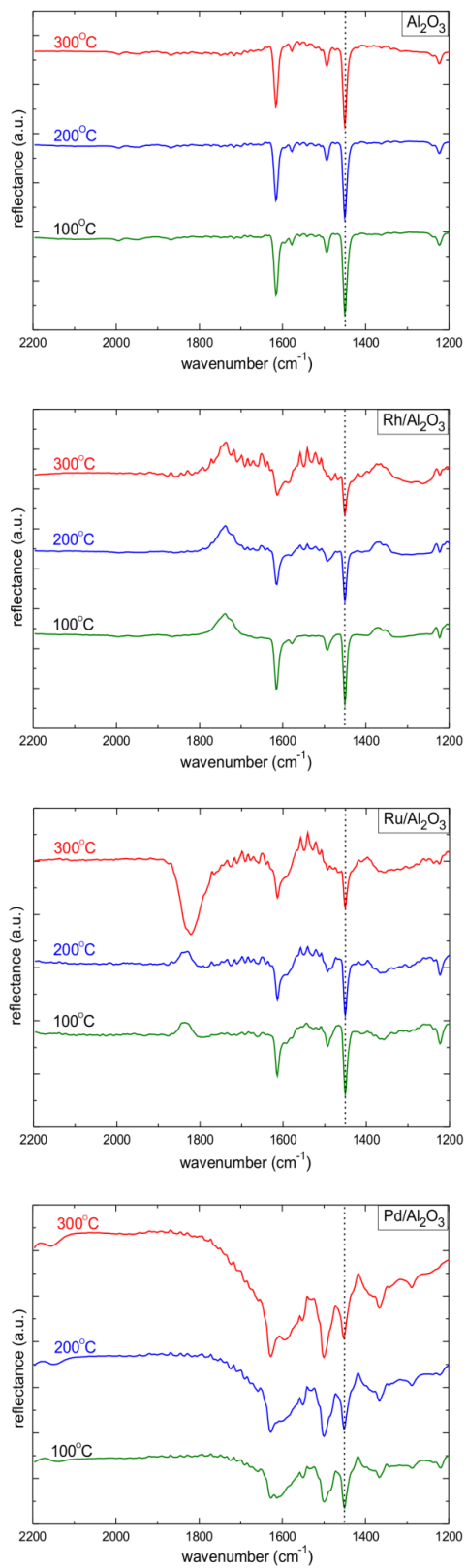


Figure S1: DRIFT spectra of pyridine adsorbed on Al_2O_3 , $\text{Rh}/\text{Al}_2\text{O}_3$, $\text{Ru}/\text{Al}_2\text{O}_3$, and $\text{Pd}/\text{Al}_2\text{O}_3$.

Table S1: Analysis of the variance (ANOVA) of the built linear models

System-Product Yield (%)	Source of Variation	Degrees of Freedom	Summ of squares	Mean squares	F statistic	p-value
Pd ^a -Oil Yield (%)	Regression	3	1408.10	469.37	2.51	0.235
	Error	3	560.19	186.73		
	Total	6	1968.29			
Pd ^a -Solid Yield (%)	Regression	3	2011.10	670.35	3.25	0.180
	Error	3	619.00	206.33		
	Total	6	2630.10			
Rh ^b -Oil Yield (%)	Regression	3	1141.60	380.55	2.20	0.267
	Error	3	518.09	172.70		
	Total	6	1659.69			
Rh ^b -Solid Yield (%)	Regression	3	1757.10	585.71	3.83	0.150
	Error	3	458.83	152.94		
	Total	6	2215.93			
Ru ^c -Oil Yield (%)	Regression	3	1833.00	611.02	1.83	0.315
	Error	3	999.32	333.11		
	Total	6	2832.32			
Ru ^c -Solid Yield (%)	Regression	3	2211.10	737.03	4.41	0.127
	Error	3	501.17	167.06		
	Total	6	2712.27			

a) ANOVA analysis for the Pd/Al₂O₃ system b) ANOVA analysis for the Rh/Al₂O₃ system c) ANOVA analysis for the Ru/Al₂O₃ system

Table S2: ANOVA table for the second order regression models

System	Source of Variation	Degrees of Freedom	Summ of squares	Mean squares	F statistic	p-value
NC ^a Oil Yield (%)	Regression	5	2318.30	463.65	4.01	0.077
	Error	5	578.13	115.63		
	Total	10	2896.43			
NC ^a Solid Yield (%)	Regression	5	4443.80	888.77	5.35	0.045
	Error	5	830.38	166.08		
	Total	10	5274.18			
Ru ^b Oil Yield (%)	Regression	5	4398.00	879.60	7.12	0.025
	Error	5	617.79	123.56		
	Total	10	5015.79			
Ru ^b Solid Yield (%)	Regression	5	6197.10	1239.40	17.24	0.004
	Error	5	359.47	71.89		
	Total	10	6556.57			
Al ^c Oil Yield (%)	Regression	5	2892.90	578.59	5.05	0.050
	Error	5	572.39	114.48		
	Total	10	3465.29			
Al ^c Solid Yield (%)	Regression	5	4698.30	939.66	7.59	0.022
	Error	5	619.02	123.80		
	Total	10	5317.32			

a) ANOVA analysis for the non-catalysed system b) ANOVA analysis for the Ru/Al₂O₃ system c) ANOVA analysis for the γ -Al₂O₃ system